



Synthesis and characterization of Znq2 and Znq2:CTAB particles for optical applications

V BHARATHI DEVI^{1,2}, P ARULMOZHICHELVAN¹ and P MURUGAKOOTHAN^{1,*}

¹MRDL, PG and Research Department of Physics, Pachaiyappa's College, Chennai 600 030, India

²Department of Physics, Dr M.G.R. Educational and Research Institute University, Chennai 600 095, India

*Author for correspondence (murugakoothan03@yahoo.co.in)

MS received 24 June 2016; accepted 25 January 2017; published online 12 September 2017

Abstract. High luminescent zinc (ii)-bis (8-hydroxyquinoline) Znq2 nanoparticles were synthesized by the simple precipitation method in pure form and with cetyltrimethyl ammonium bromide (CTAB) as cationic surfactant. The crystalline nature of title samples was confirmed by powder X-ray diffraction. Thermo gravimetric analysis and differential thermal analysis were carried out to find the thermal stability of the synthesized samples. The morphology and elemental analyses of the samples were studied by scanning electron microscope and energy dispersive X-ray analyser, respectively. The functional groups of these nanoparticles were analysed and assigned using the Fourier transform infrared spectroscopy spectral study. The optical property of Znq2 and Znq2:CTAB was confirmed by UV-vis-NIR spectral study. The band gap of Znq2 was calculated. The synthesized Znq2 and Znq2:CTAB nanoparticles were confirmed by photoluminescence studies for organic-light-emitting diode applications as emission and electron transport layers.

Keywords. Znq2:CTAB; nanoparticles; thermal stability; SEM; FTIR; UV-vis-NIR.

1. Introduction

Luminescent organic/organo metallic compounds have been attracting much attention in recent years because of their potential application in flat panel displays based on organic-light-emitting diodes (OLEDs) [1–3]. Luminescent chelate complexes have shown to be particularly useful in OLEDs because of their relatively high stability and efficiency [4–7]. Among these materials, zinc (ii)-bis (8-hydroxyquinoline) (Znq2) has been widely used as an emissive as well as electron transporting material in organic-light-emitting diodes. Znq2 is used as an emissive transport material because of its excellent electron transport properties; this is due to the better $\pi-\pi$ overlap of molecular orbital of the zinc derivatives. In this article, a systematic investigation has been carried out to synthesize Znq2 particles by a simple precipitation method. As a result, this study sets out to evaluate the structure, optical and thermal properties of znq2 particles. Surface modification of the particles has been carried out using ionic surfactant of cetyltrimethyl ammonium bromide (CTAB).

2. Materials and methods

2.1 Materials

Zinc acetate ($\text{ZnC}_4\text{H}_6\text{O}_4$), 8-hydroxyquinoline (8Hq) and ammonia (NH_3), all of Merck brand, were used as the starting materials. All these chemicals were of high purity and

no further purification was done. N-cetyl-N, N, N-trimethyl ammonium bromide (CTAB) was used as the surfactant.

2.2 Synthesis of Znq2 nanoparticles

The Znq2 nanoparticles were synthesized by the simple precipitation method using zinc acetate, 8-Hq and NH_3 in the stoichiometric ratio 1:2:1. A solution of 8-Hq (5.442 g) was prepared using the mixed solvent of NH_3 (0.04 ml) and double distilled water. The solution was stirred with a magnetic stirrer to attain homogenization and it was used as a reaction mixture. An aqueous solution of zinc acetate (4.3175 g) was added drop-wise to the reaction mixture, which yields a yellowish precipitate. The yellow precipitate was filtered and washed several times with distilled water and dried in a vacuum oven for 6 h. The sample was named as sample (a).

2.3 Synthesis of Znq2 nanoparticles with CTAB

Initially zinc acetate (4.3175 g) was dissolved in 100 ml of water and stirred using a magnetic stirrer for 1 h at room temperature. In this solution, 0.03435 g of CTAB dissolved in 20 ml of water was added. The 8 Hq solution was separately prepared by dissolving 5.442 g of 8 Hq in a mixed solvent of NH_3 (0.04 ml) and water (100 ml) and then it was added drop by drop to the above solution under continuous stirring. The yellow precipitate was formed immediately. The yellow precipitate was filtered and washed several times with distilled

water and dried in a vacuum oven for 6 h. The synthesized material was named as sample (b).

2.4 Characterization studies

Powder X-ray diffraction (PXRD) analysis was carried out using a Rich Seifert X-ray diffractometer with Cu $K\alpha$ ($\lambda = 1.5418 \text{ \AA}$) radiation. The thermo gravimetric analysis and differential thermal analysis (TG–DTA) thermograms of the samples were recorded using a SEIKO DSC200 instrument under nitrogen atmosphere at a heating rate of $10^\circ\text{C min}^{-1}$. Scanning electron microscope (SEM) was employed for morphological study using a CARI ZEISS MA15/EVO18 operated at 30 kV with energy dispersive X-ray analyser (EDAX). The Fourier transform infrared spectroscopy (FTIR) spectra of Znq2 and Znq2:CTAB nanoparticles were recorded in the range of $4000\text{--}400 \text{ cm}^{-1}$ employing a BRUKER 66 V FTIR spectrometer using the KBr pellet method to study the metal complex co-ordination. The optical absorption spectra of the samples were recorded in the range of $200\text{--}800 \text{ nm}$ using double beam CARY 5E UV–vis–NIR spectrophotometer. The photoluminescence (PL) study was done using a JOBIN YVON FLUROLOG-3-11 spectrofluorometer with an excitation wavelength (λ_{ex}) of 380 nm.

3. Results and discussion

3.1 Powder X-ray diffraction analysis

The PXRD patterns of Znq2 and Znq2:CTAB are shown in figure 1. The sharp diffraction peaks observed in figure 1a for Znq2 confirms the good crystalline nature of the sample.

The precipitation method followed in this work yields a good crystalline-natured sample due to the availability of sufficient time for the formation of small crystalline samples. In the case of Znq2:CTAB, figure 1b, a few diffraction peaks are produced from the amorphous background suggesting that the synthesized powder is a mixture of crystalline and amorphous phase. This is due to the interaction between Znq2 molecule and the oxygen atom in the CTAB [8]. The lattice parameters, from the powder XRD pattern, are evaluated and peak indexing was carried out using the software Proszki Version 2.4.

3.2 Thermal analysis

Thermal stability of the particles was determined by the TG and DTA unit of SEIKO model TG/DTA 6200. The TG and DTA thermograms of the synthesized Znq2 nanoparticle are shown in figure 2a. The TG thermogram shows three stages of weight loss of Znq2. The first stage occurs from 164 to 207°C with the weight loss of 41.3% . The second stage occurs from 207 to 443°C with the weight loss of 15.6% . The third stage occurs from 443 to 558°C with the weight loss of 27.1% . From the TG curve it is clear that the sample is stable up to 164°C . The endothermic peak observed in DTA thermogram at 201°C coincides with the first stage weight loss of Znq2. The observed endothermic peak of Znq2 is attributed to the absorption of energy for breaking of bonds during decomposition. Figure 2b shows the thermal analysis of Znq2:CTAB and it shows that the sample is stable up to 156°C . From the thermal analysis it is evident that the Znq2 sample has higher thermal stability compared to Znq2:CTAB. This may be due to the fact that the surfactant CTAB attached to the Znq2 leads to the lower thermal stability of the Znq2.

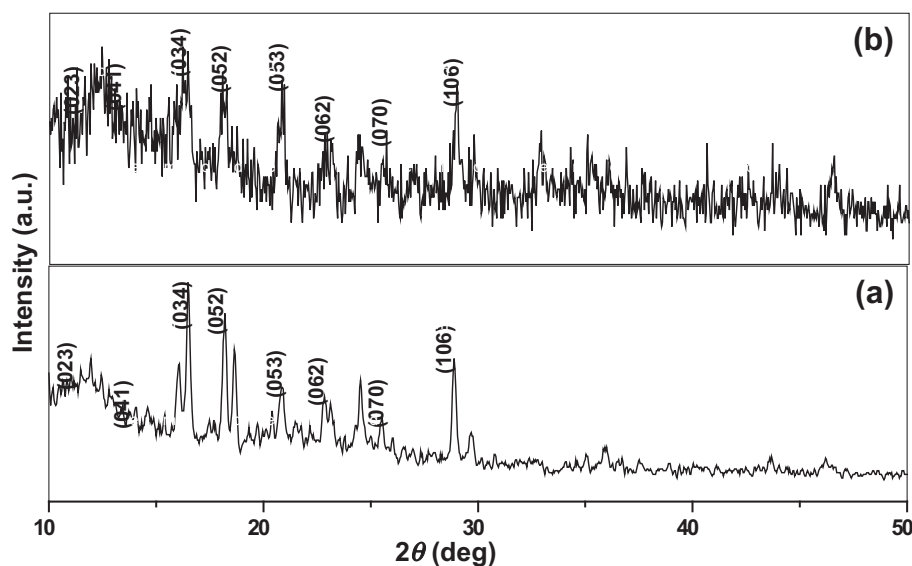


Figure 1. PXRD patterns of (a) Znq2 and (b) Znq2:CTAB.

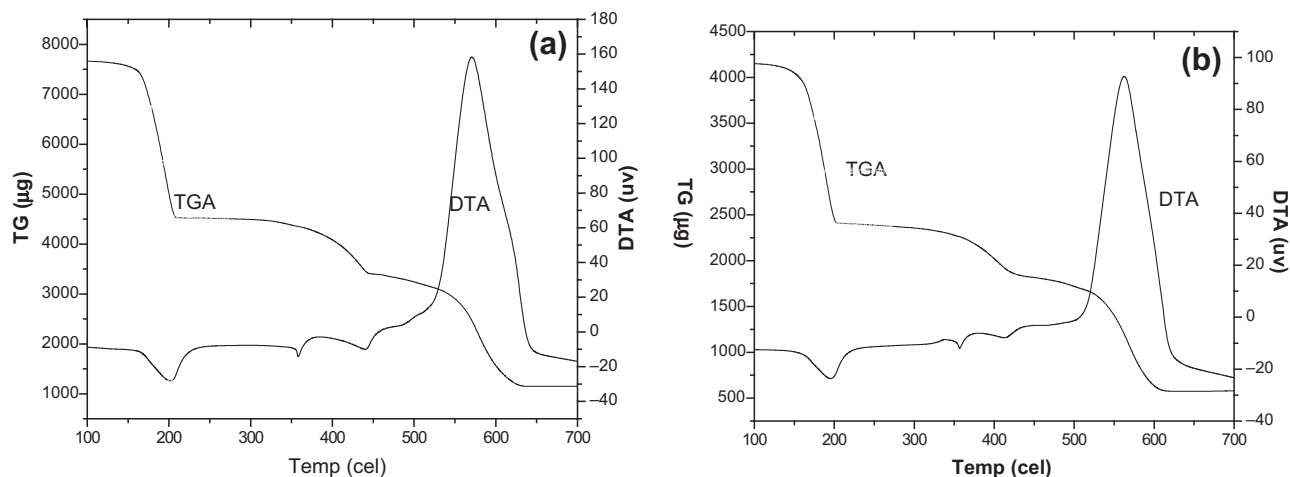


Figure 2. Thermal analyses of (a) Znq2 and (b) Znq2:CTAB.

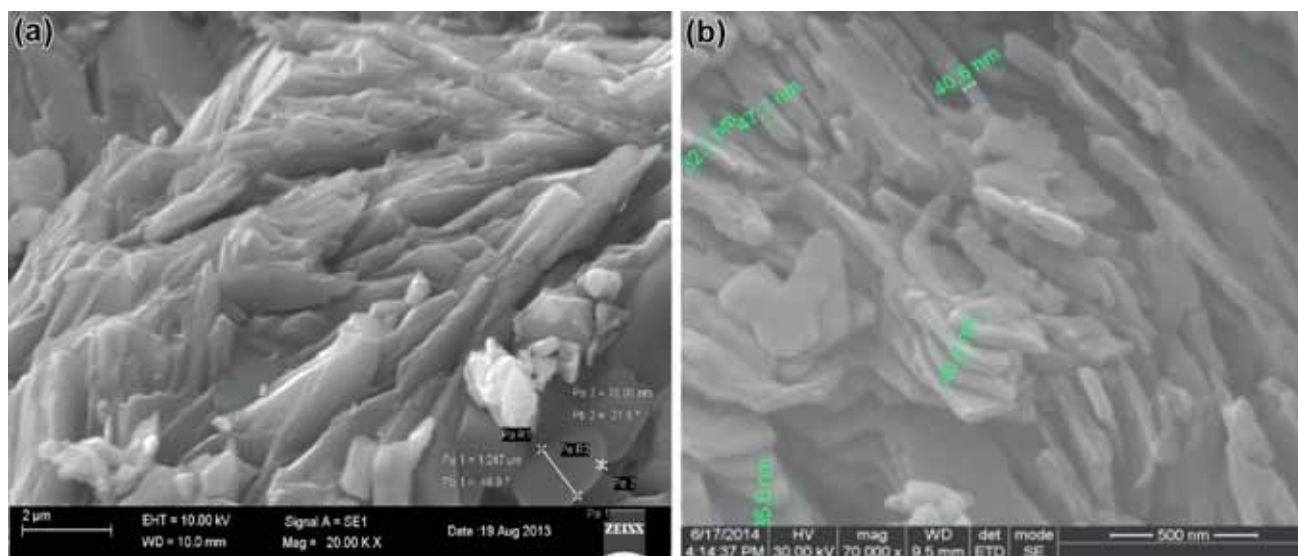


Figure 3. SEM images of (a) Znq2 and (b) Znq2:CTAB.

3.3 SEM analysis

Scanning electron microscope image of Znq2 particles is shown in figure 3a. Nano sheet-like layers were found with a maximum thickness of about 78.88 nm. The thickness of the Znq2:CTAB nanoparticles were found with a maximum thickness of 40 nm, as shown in figure 3b. The reduction in the thickness of the Znq2:CTAB nanoparticles may be attributed to that CTAB, which affects the process of nucleation and growth of crystallites during synthesis.

3.4 EDAX analysis

The EDAX spectrum for the Znq2 particles, shown in figure 4a, revealed the presence of Zn and O as the only elementary species in the sample. Figure 4b shows the

EDAX spectrum of Znq2:CTAB particles in which there is an additional peak corresponding to bromide. The bromide peak confirms the presence of CTAB with Znq2.

3.5 FTIR spectroscopic analysis

The FTIR spectrum of Znq2 nanoparticles was recorded in the range of 4000–400 cm^{-1} employing a BRUKER 66 V FTIR spectrometer and using the KBr pellet technique. The FTIR spectrum of Znq2, Znq2:CTAB are shown in figure 5a and b. The vibrations at 1604, 1577 and 1327 cm^{-1} are assigned to the quinoline group of Znq2. The bands at 1499 and 1467 cm^{-1} correspond to both the pyridyl and phenyl groups in Znq2. The peaks at 743 and 642 cm^{-1} are associated with in-plane ring deformation [9–11]. The absorption peaks at 2852 and 2923 cm^{-1} correspond to the stretching modes of

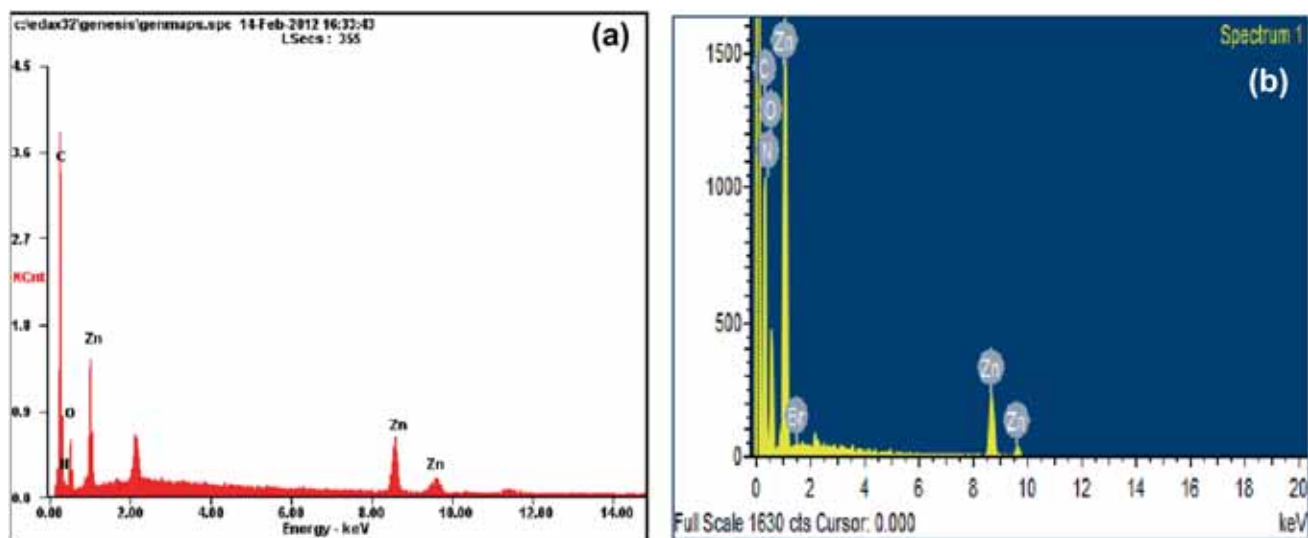


Figure 4. EDAX spectrum of (a) Znq2 and (b) Znq2:CTAB.

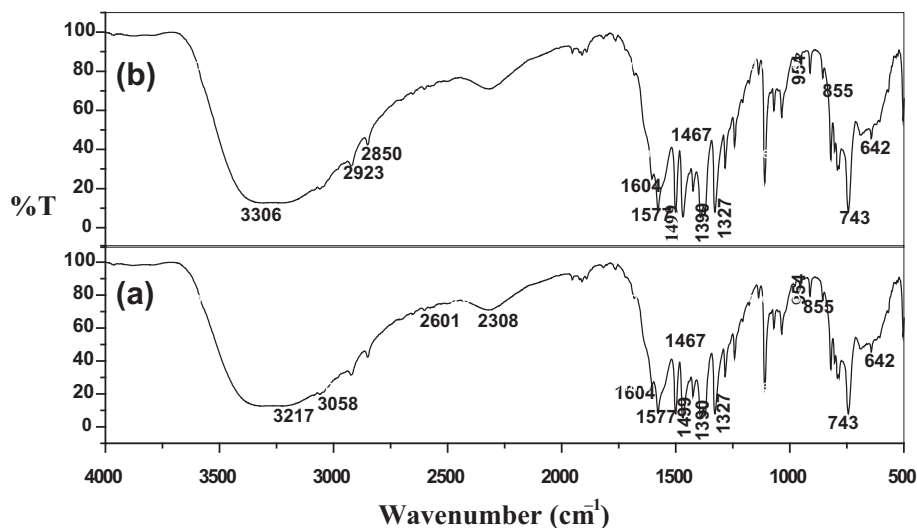


Figure 5. FT-IR spectrum of (a) Znq2 and (b) Znq2:CTAB.

methylene groups, which confirm the presence of CTAB with Znq2 [12].

3.6 UV-vis-NIR spectral analysis

The UV-vis-NIR absorption spectra of Znq2 particles are shown in figure 6a. Two absorption peaks are observed, one at 245 nm and another low intensity peak at 314 nm at the band gap of 3.5 eV. Figure 6b shows the absorption spectra of Znq2:CTAB. The shift of the peaks observed for the Znq2:CTAB nanoparticles can be assigned to the presence of CTAB with Znq2. The peaks observed are at 267 nm and another low intensity peak at 382 nm at the band gap of 3.25 eV for

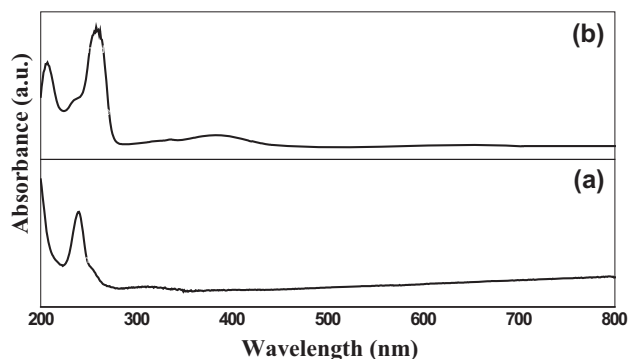


Figure 6. Absorption spectrum of (a) Znq2 and (b) Znq2:CTAB.

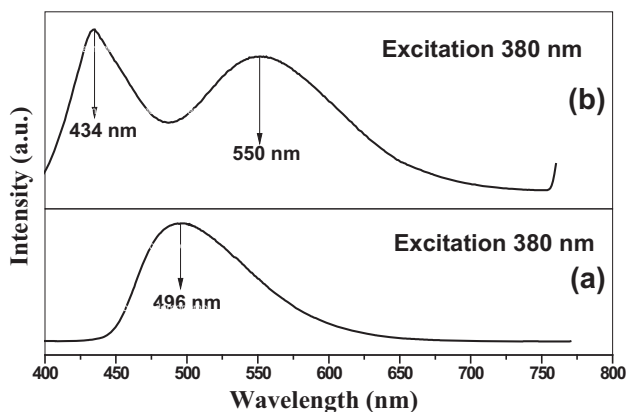


Figure 7. Photoluminescence spectra of (a) Znq2 and (b) Znq2:CTAB.

Znq2:CTAB. The low intensity peaks in all the compounds are assigned as $\pi-\pi^*$ electronic transitions [13–15].

3.7 PL analysis

The PL spectrum of Znq2 particles in the excitation wavelength of 380 nm is shown in figure 7a, which shows a strong and broad emission band at 496 nm in the bluish green region. The PL spectrum of Znq2:CTAB is shown in figure 7b at the excitation wavelength of 380 nm. Two emission peaks are observed at 434 nm (blue) and 550 nm (green). The emission peak at 434 nm corresponds to the band–edge emission. The green emission peak at 550 nm arises from the singly ionized oxygen vacancy due to the recombination of a photo-generated hole with a singly ionized electron in the valance band [16,17]. Emission can be assigned to $\pi-\pi^*$ transition localized on the quinoline rings. The PL emission of the Znq2:CTAB was red shifted by 54 nm from the PL emission of the Znq2. The red shift in the PL of the Znq2:CTAB suggested that there is significant delocalization of $\pi-\pi^*$ transition of the excited state due to the presence of CTAB [8]. From the above discussion it is clear that Znq2:CTAB is not only suitable for optical but for other applications as well [18].

4. Conclusions

Simple precipitation method has been presented to synthesize pure and CTAB-assisted Znq2 particles. The

properties of Znq2 particles were studied by the XRD, thermal analyses, SEM, EDAX, FTIR, UV–vis–NIR and PL analysis. The SEM analyses showed that the average particle size of the znq2 is reduced due to the effect of the surfactant. Our investigations indicated that the CTAB-assisted Znq2 particles are the best in terms of size, morphology, structure and optical properties. Znq2 and Znq2:CTAB are considered as novel electroluminescence materials for OLED applications. It can be concluded that the synthesized Znq2 nanoparticles are useful for applications in organic-light-emitting devices.

References

- [1] Tang C W and Van Slyke S A 1987 *Appl. Phys. Lett.* **51** 913
- [2] Tang C W, Van Slyke S A and Chen C H 1989 *J. Appl. Phys.* **65** 3610
- [3] Rahulkumar Singh K, Srivastava R and Kamlasanan M N 2011 *J. Nano. Electron. Phys.* **3** 514
- [4] Adachi C, Tokito S, Tsutsui T and Saito S 1988 *Jpn. J. Appl. Phys.* **27** 713
- [5] Burroughes J H, Bradley D D C and Brown A R 1990 *Nature* **347** 539
- [6] Sheats J R, Antoniadis H and Hueschen M 1996 *Science* **5277** 884
- [7] Trinh Dac Hoanh, Young HoonIm, Dong-EunKim, Young-SooKwon and Burm-Jong Lee 2012 *J. Nanomater.* **2012** 7
- [8] Nagpure I M, Duvenhage, Shreyas M M, Pitale S, Ntwaeaborwa O M, Terblans J J *et al* 2012 *J. Fluoresc.* **22** 1271
- [9] Hong-Cheng Pan, Fu-Pei Liang, Chang-Jie Mao, Jun-Jie Zhu and Hong-Yuan Chen 2007 *J. Phys. Chem. B* **111** 5767
- [10] Vivek K S and Jaya M 2013 *J. Mater.* **2013** 5
- [11] Shao Q, Wang T, Wang X and Chen Y 2011 *Front. Optoelectron. China* **4** 195
- [12] Jesuvathy S D and Murugakoothan P 2013 *Int. J. Enhanced Res. Sci. Technol. Eng.* **3** 414
- [13] Nishal V, Kumar A, Kadyan P S, Singh D, Srivastava R, Singh *et al* 2013 *J. Electron. Mater.* **42** 973
- [14] Mahmoud M E, Haggag S S and Abdel-Fattah T M 2009 *Polyhedron* **28** 181
- [15] Monzon L M A, Burke F and Coey J M D 2011 *J. Phys. Chem. C* **115** 9182
- [16] Amrut, Lanje S, Satish, Sharma J, Ramchandara, Pode B *et al* 2010 *Adv. Appl. Sci. Res.* **1** 36
- [17] Viswanatha R, Arthoba Nayak Y, Venkatesha T G and Vidyasagar C C 2013 *An International Journal* **3** 16
- [18] Michael C, Jurgen G, Wolfgang M, Harald H and Wolfgang B 2003 *Adv. Funct. Mater.* **13** 108